Self-consistent continuum solvation for optical absorption of complex molecular systems in solution

ARTICLE *in* THE JOURNAL OF CHEMICAL PHYSICS · JANUARY 2015

Impact Factor: 2.95 · DOI: 10.1063/1.4905604 · Source: PubMed

5 AUTHORS, INCLUDING:

Iurii Timrov
Scuola Internazionale Superiore di Studi Av…
8 PUBLICATIONS **45** CITATIONS
SEE PROFILE

Oliviero Andreussi
University of Lugano
20 PUBLICATIONS **220** CITATIONS
SEE PROFILE

Alessandro Biancardi
11 PUBLICATIONS **181** CITATIONS
SEE PROFILE

Stefano Baroni
Scuola Internazionale Superiore di Studi Av…
245 PUBLICATIONS **17,126** CITATIONS
SEE PROFILE

Self-consistent continuum solvation for optical absorption of complex molecular systems in solution

Iurii Timrov, Oliviero Andreussi, Alessandro Biancardi, Nicola Marzari, and Stefano Baroni

Citation: The Journal of Chemical Physics **142**, 034111 (2015); doi: 10.1063/1.4905604
View online: http://dx.doi.org/10.1063/1.4905604
View Table of Contents: http://scitation.aip.org/content/aip/journal/jcp/142/3?ver=pdfcov
Published by the AIP Publishing

Self-consistent continuum solvation for optical absorption of complex molecular systems in solution

Iurii Timrov,[1] Oliviero Andreussi,[2] Alessandro Biancardi,[1] Nicola Marzari,[3] and Stefano Baroni[1,3,a)]

[1]*SISSA – Scuola Internazionale Superiore di Studi Avanzati, Via Bonomea 265, 34136 Trieste, Italy*
[2]*Dipartimento di Chimica e Chimica Industriale, Università di Pisa, Via Risorgimento 35, Pisa 56126, Italy*
[3]*Theory and Simulation of Materials (THEOS), École Polytechnique Fédérale de Lausanne, 1015 Lausanne, Switzerland*

(Received 9 October 2014; accepted 24 December 2014; published online 16 January 2015)

We introduce a new method to compute the optical absorption spectra of complex molecular systems in solution, based on the Liouville approach to time-dependent density-functional perturbation theory and the revised self-consistent continuum solvation model. The former allows one to obtain the absorption spectrum over a whole wide frequency range, using a recently proposed Lanczos-based technique, or selected excitation energies, using the Casida equation, without having to ever compute any unoccupied molecular orbitals. The latter is conceptually similar to the polarizable continuum model and offers the further advantages of allowing an easy computation of atomic forces via the Hellmann-Feynman theorem and a ready implementation in periodic-boundary conditions. The new method has been implemented using pseudopotentials and plane-wave basis sets, benchmarked against polarizable continuum model calculations on 4-aminophthalimide, alizarin, and cyanin and made available through the Quantum ESPRESSO distribution of open-source codes. © *2015 AIP Publishing LLC.* [http://dx.doi.org/10.1063/1.4905604]

I. INTRODUCTION

The optical properties of molecular systems crucially depend on the chemico-physical conditions (composition, temperature, acidity, etc.) of the solvent in which they are dissolved. While these effects can in principle be addressed by treating solvent molecules on a par with the solvated one,[1] all the approaches based on an explicit quantum-mechanical treatment of the solvent are extremely costly, and by their very nature, they can only be applied to a small number of rather simple systems. Screening many different molecules for desired optical properties and/or understanding the effects of complex molecular interactions (such as, e.g., copigmentation) call for new methods that, while being substantially less expensive than explicit solvent models, maintain a comparable level of accuracy.

Continuum solvation models,[2] such as the *polarizable continuum model* (PCM)[3–7] or the *conductor-like screening model* (COSMO),[8] have proven to be very effective in accounting for the complexity of the solvent-solute interactions in an implicit fashion. In PCM, the solvent is represented by a classical continuous medium—described by its experimental macroscopic dielectric constant—that is assumed to be homogeneous but for a void cavity hosting the solvated molecule. In spite of its simplicity, PCM has proved to be rather successful in accounting for the electrostatic effects of the polarization charge induced in the solvent by the solute on the equilibrium and dynamical properties of the latter.[2,7] Its main practical drawbacks are that the discontinuity of the cavity makes the computation of electrostatic potentials cumbersome and not easily implemented in periodic-boundary conditions, and that its shape and size are input of the model (usually, a superposition of atom-centered spheres), which prevents a straightforward use of the Hellmann-Feynman theorem to compute atomic forces.

These difficulties are addressed, and to a large extent overcome, by a recently proposed revised[9–11] *self-consistent continuum solvation* (SCCS) model,[12–15] in which the hosting medium is defined in such a way that the interface between the solvent and the cavity hosting the solute is smooth and determined self-consistently by the ground-state electronic charge-density of the latter.

PCM has been extended to describe electronic excitations,[16–18] in particular, in the framework of the linear-response time-dependent (TD) Hartree-Fock,[19] density-functional theory (DFT),[20,21] and coupled-cluster theories.[22,23] In these formulations, an additional difficulty arises in that the ionic and electronic degrees of freedom of the solvent respond differently to a perturbation of optical frequency, as reflected by the frequency dependence of its dielectric function. In the off-resonance case (i.e., when the solvent does not absorb at the frequencies where the solute does), it is often sufficient to assume that the solvent is described by its high-frequency dielectric constant, ϵ_∞, rather than by the static one, ϵ_0.

In this work, a similar goal is pursued by combining a linearization of the SCCS model with the Liouville approach to TD density-functional perturbation theory (TDDFpT), in both its Lanczos[24–26] and Casida-Davidson[27] flavors. This combination provides a consistent scheme where electrostatic effects and atomic forces are evaluated for the ground state in

a)Electronic address: baroni@sissa.it

periodic-boundary conditions, using the former methodology, and molecular excitation spectra are computed over extended frequency ranges, using the latter.

Both implicit and explicit models for the solvent have limitations and strengths, which are worth briefly mentioning here. First, an explicit molecular description of the solvent allows to model with greater accuracy short-range solvent-solute interactions—this is, e.g., relevant when solvent molecules (usually from the first solvation shell) participate in the electronic transitions of the solute (see, e.g., Ref. 28), or when the thermal bath of the solvent affects directly the configurational ensemble averages of the solute. On the other hand, the theoretical description of the dielectric properties of the solvent, based on current first-principles techniques, can be fairly inaccurate. This is mostly the case for static dielectric screening, that e.g., for water is affected by a combination of an overestimated resilience of the hydrogen-bond network (also resulting in too high a melting temperature) and an oversampling of local ferroelectric configurations. Implicit solvents can impose instead the correct, temperature-dependent screening. Mixed models,[29,30] then, where the first solvation shells are described explicitly, and the rest is implicit, could probably offer the optimal balance for ultimate accuracy.

This paper is organized as follows: in Sec. II, we recall the fundamentals of the SCCS model and present the equations that, upon linearization within the Liouville approach to TDDFpT, allow one to compute the molecular dynamical polarizability in solution; in Sec. III, we report on a benchmark of our method, as implemented in the QUANTUM ESPRESSO suite of plane-wave (PW) pseudopotential codes,[31] that we have made for 3 molecules (4-aminophthalimide (4-AP), alizarin, and cyanin), against PCM results, obtained from the GAUSSIAN code;[32] our conclusions are finally presented in Sec. IV.

II. THEORY

A. The SCCS model

1. Electrostatics

In the spirit of PCM, the SCCS model represents the solvent by a dielectric medium, characterised by a dielectric constant ϵ_0, that is homogeneous but for a void cavity hosting the solute. While in PCM, the shape of the cavity is fixed as a superposition of atom-centered spheres, thus making the dielectric medium discontinuous at the surface of the atomic spheres; in SCCS, it is smooth and determined self-consistently by the electronic charge-density distribution of the solute, $n_e^\circ(\mathbf{r})$. This is achieved by defining an effective local dielectric constant as

$$\epsilon(\mathbf{r}) = \eta(n_e^\circ(\mathbf{r}), \bar{\epsilon}), \tag{1}$$

where

$$\eta(n_e^\circ(\mathbf{r}), \bar{\epsilon}) = \begin{cases} 1 & n_e^\circ(\mathbf{r}) > n_{max} \\ t(n_e^\circ(\mathbf{r}), \bar{\epsilon}) & n_{min} < n_e^\circ(\mathbf{r}) < n_{max}, \\ \bar{\epsilon} & n_e^\circ(\mathbf{r}) < n_{min} \end{cases} \tag{2}$$

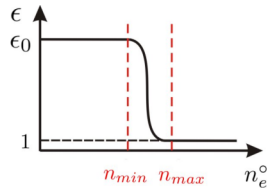

FIG. 1. Schematic illustration of the ground-state dielectric function ϵ, defined by Eq. (2), as a function of the ground-state electronic density $n_e^\circ(\mathbf{r})$. Here, ϵ_0 is the static dielectric constant of the solvent, n_{min} and n_{max} are the fitting parameters of the SCCS model which control the smoothness of the interface between the solute and the solvent.

$t(n, \bar{\epsilon})$ is a function that interpolates smoothly between the values $\bar{\epsilon}$ and 1, and n_{min} and n_{max} are fitting parameters that control the smoothness of the interface, as illustrated in Fig. 1. The constant $\bar{\epsilon}$ in Eq. (2) is whatever the dielectric constant appropriate to the problem at hand. In ground-state applications, it is conveniently set to the static dielectric constant of the solvent $\bar{\epsilon} = \epsilon_0$, whereas, when dealing with excited-state properties, it is often appropriate to assume that it coincides with the high-frequency dielectric constant, $\bar{\epsilon} = \epsilon_\infty$ (see Sec. II B 1). In this work, we adopt the form of $t(n, \bar{\epsilon})$ proposed in Ref. 9

$$t(n,\bar{\epsilon}) = \exp\left\{\frac{\ln\bar{\epsilon}}{2\pi}\left[2\pi\frac{\ln n_{max} - \ln n}{\ln n_{max} - \ln n_{min}} - \sin\left(2\pi\frac{\ln n_{max} - \ln n}{\ln n_{max} - \ln n_{min}}\right)\right]\right\}. \tag{3}$$

The parameters n_{min} and n_{max} were determined by fitting total electrostatic energy of the SCCS model to the one obtained from PCM for a large set of neutral molecules in water and fixed to the values of 0.0001 a.u. and 0.005 a.u., respectively.[9] The relation between the ground-state electronic charge-density of the solute and the continuous medium describing the solvent is illustrated in Fig. 2. In the presence of a polarizable medium described by the dielectric constant of Eq. (2), the total electrostatic potential satisfies a Poisson-like equation, reading

$$\nabla\cdot\left(\epsilon(\mathbf{r})\nabla V_{\text{tot}}^\circ(\mathbf{r})\right) = -4\pi n_{\text{m}}^\circ(\mathbf{r}), \tag{4}$$

where $n_{\text{m}}^\circ(\mathbf{r})$ is the total (electronic plus ionic) ground-state charge-density of the solute,

$$n_{\text{m}}^\circ(\mathbf{r}) = n_{\text{e}}^\circ(\mathbf{r}) + n_{\text{i}}^\circ(\mathbf{r}), \tag{5}$$

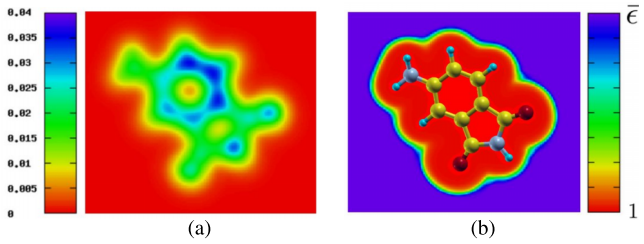

FIG. 2. Panel (a): Intensity map of the ground-state electronic charge-density distribution $n_e^\circ(\mathbf{r})$ of the 4-AP molecule. Panel (b): Intensity map of the dielectric function defined by Eqs. (2) and (3). The dielectric function is equal to 1 inside the cavity and to $\bar{\epsilon}$ outside the cavity ($\bar{\epsilon} = \epsilon_0$ for the ground state and $\bar{\epsilon} = \epsilon_\infty$ for the excited state).

$n_{\rm i}^{\circ}(\mathbf{r})$ being the ionic density of the solute, which can be represented as a sum of Gaussian functions centered on the nuclei of the molecule and $V_{\rm tot}^{\circ}(\mathbf{r})$ is the total ground-state electrostatic potential of the solvated system. Equation (4) is non-linear because the dielectric function appearing on its left-hand side depends on the electronic density of the solute, see Eqs. (2) and (3), which is in turn determined by the electrostatic potential that is solution to it, through the quantum-mechanical Kohn-Sham (KS) equations reported in Sec. II A 2. For this reason, it can be solved iteratively like a *self-consistent* problem, whence the name of the model. We stress that, while in the full SCCS model, additional terms proportional to the *quantum volume* and *quantum surface*[33] are introduced to deal with solute free energies, here, only dielectric screening is retained in the SCCS (dielectric SCCS model).

For computational purposes, it is convenient to define a polarization density $n_{\rm p}^{\circ}(\mathbf{r})$ and to map the effect of the dielectric onto it.[9] This allows us to rewrite Eq. (4) in the form of an ordinary Poisson equation in vacuum

$$\nabla^2 V_{\rm tot}^{\circ}(\mathbf{r}) = -4\pi\left(n_{\rm m}^{\circ}(\mathbf{r}) + n_{\rm p}^{\circ}(\mathbf{r})\right), \tag{6}$$

where the ground-state polarization density $n_{\rm p}^{\circ}(\mathbf{r})$ reads[9]

$$n_{\rm p}^{\circ}(\mathbf{r}) \equiv \frac{1}{4\pi}\nabla\ln\epsilon(\mathbf{r})\cdot\nabla V_{\rm tot}^{\circ}(\mathbf{r}) - \frac{\epsilon(\mathbf{r})-1}{\epsilon(\mathbf{r})}n_{\rm m}^{\circ}(\mathbf{r}). \tag{7}$$

The solution to Eq. (4) can be conveniently split into a sum of ionic, electronic, and polarization contributions, as: $V_{\rm tot}^{\circ}(\mathbf{r}) = V_{\rm i}^{\circ}(\mathbf{r}) + V_{\rm e}^{\circ}(\mathbf{r}) + V_{\rm p}^{\circ}(\mathbf{r})$.

The dielectric SCCS model can be applied to different quantum-mechanical approaches, but in Sec. II A 2, we specialize our discussion to the case of KS DFT.[34,35]

2. Quantum mechanics

The ground-state KS equation for the solvated molecule reads

$$\hat{H}_{\rm KS}^{\circ}\varphi_v^{\circ}(\mathbf{r}) = \varepsilon_v^{\circ}\varphi_v^{\circ}(\mathbf{r}), \tag{8}$$

where v is an electron-state index, $\varphi_v^{\circ}(\mathbf{r})$ and ε_v° are KS orbitals and energies, respectively, and $\hat{H}_{\rm KS}^{\circ}$ is the KS Hamiltonian which reads (hereafter, we use Hartree atomic units: $\hbar = m = e = 1$)

$$\hat{H}_{\rm KS}^{\circ} = -\frac{1}{2}\nabla^2 + V_{\rm KS}^{\circ}(\mathbf{r}), \tag{9}$$

$V_{\rm KS}^{\circ}(\mathbf{r})$ being the ground-state KS effective potential,

$$V_{\rm KS}^{\circ}(\mathbf{r}) = V_{\rm ext}^{\circ}(\mathbf{r}) + V_{\rm int}^{\circ}(\mathbf{r}). \tag{10}$$

In Eq. (10), the *external* potential acting on the electrons in the solute, $V_{\rm ext}^{\circ}(\mathbf{r})$, can be conveniently split into an ionic electrostatic long-range contribution, $V_{\rm i}^{\circ}(\mathbf{r})$, and a short-range (possibly non-local) contribution due to the pseudopotential approximation, $V_{\rm SR}^{\circ}(\mathbf{r})$

$$V_{\rm ext}^{\circ}(\mathbf{r}) = V_{\rm i}^{\circ}(\mathbf{r}) + V_{\rm SR}^{\circ}(\mathbf{r}). \tag{11}$$

The *internal* contribution to the KS potential in Eq. (10), $V_{\rm int}^{\circ}(\mathbf{r})$, reads

$$V_{\rm int}^{\circ}(\mathbf{r}) = V_{\rm e}^{\circ}(\mathbf{r}) + V_{\rm p}^{\circ}(\mathbf{r}) + V_{\epsilon}^{\circ}(\mathbf{r}) + V_{\rm XC}^{\circ}(\mathbf{r}), \tag{12}$$

where $V_{\rm e}^{\circ}(\mathbf{r})$ is the electronic Hartree (electrostatic) potential

$$V_{\rm e}^{\circ}(\mathbf{r}) = \int \frac{n_{\rm e}^{\circ}(\mathbf{r}')}{|\mathbf{r}-\mathbf{r}'|}\,d\mathbf{r}', \tag{13}$$

where $n_{\rm e}^{\circ}(\mathbf{r})$ is defined as

$$n_{\rm e}^{\circ}(\mathbf{r}) = 2\sum_{v=1}^{N_v}|\varphi_v^{\circ}(\mathbf{r})|^2, \tag{14}$$

and the factor of 2 accounts for spin degeneracy in nonpolarized systems and N_v is the number of occupied states. $V_{\rm p}^{\circ}(\mathbf{r})$ is the electrostatic potential generated by the polarization charge induced by the solute in the solvent [see Eq. (7)]

$$V_{\rm p}^{\circ}(\mathbf{r}) = \int \frac{n_{\rm p}^{\circ}(\mathbf{r}')}{|\mathbf{r}-\mathbf{r}'|}\,d\mathbf{r}'. \tag{15}$$

The smooth interface between the solute and the solvent determines an additional contribution to the KS potential of the system, which reads[9,36]

$$V_{\epsilon}^{\circ}(\mathbf{r}) = -\frac{1}{8\pi}|\nabla V_{\rm tot}^{\circ}(\mathbf{r})|^2\frac{d\eta(n,\epsilon_0)}{dn}\Big|_{n=n_{\rm e}^{\circ}(\mathbf{r})}. \tag{16}$$

Finally,

$$V_{\rm XC}^{\circ}(\mathbf{r}) = \frac{\delta E_{\rm XC}[n]}{\delta n}\Big|_{n=n_{\rm e}^{\circ}(\mathbf{r})} \tag{17}$$

is the exchange-correlation (XC) potential, defined as usual as the functional derivative of the XC functional $E_{\rm XC}[n]$ with respect to the density. Further details on the SCCS model can be found in Refs. 9–11.

B. Linearization of the dielectric embedding

1. Response dielectric function

When a solvated system is subject to a periodic time-dependent perturbation, the dielectric function that defines the effects of the solvent on the electronic properties of the solute, Eq. (2), gets to depend on the frequency of the perturbation both explicitly through the dielectric constant of the embedding medium, $\bar{\epsilon}(\omega)$, and implicitly through the frequency dependence of the embedded molecule. To leading order in the external perturbation, the dielectric function of the solvent reads

$$\begin{aligned}\epsilon(\mathbf{r},\omega) &= \eta\left(\tilde{n}_{\rm e}(\mathbf{r},\omega),\bar{\epsilon}(\omega)\right)\\ &\approx \eta\left(n_{\rm e}^{\circ}(\mathbf{r}),\bar{\epsilon}(\omega)\right) + \frac{d\eta(n,\bar{\epsilon}(\omega))}{dn}\Big|_{n=n_{\rm e}^{\circ}(\mathbf{r})}\tilde{n}_{\rm e}'(\mathbf{r},\omega),\end{aligned} \tag{18}$$

where $\tilde{n}_{\rm e}'$ is the linear response of the molecular electronic density to the external perturbation. Given the form of Eqs. (2) and (3), the linear-order term in Eq. (18) is different from zero only at the interface between the solute molecule and the solvent, and it effectively describes a variation of the shape of the cavity that is periodic in time with frequency ω. When one is interested in the optical response of a solvated molecule, the typical time scale of nuclear motion is much longer than the period of oscillation of the electronic charge, and the nuclei of both the solvent and the solute can be assumed to remain clamped at a fixed position while an electronic transition occurs. This assumption naturally leads to two important approximations: (i) the shape of the cavity

hosting the solute does not depend on the perturbation acting on it, and the linear term in Eq. (18) can thus be neglected; (ii) the solvent molecules stay clamped also far from the interface with the cavity, and the resulting dielectric constant of the solvent coincides therefore with its high-frequency value, $\bar{\epsilon}(\omega) = \epsilon_\infty$. With these two approximations, the dynamical dielectric function of the solvent has the same form as in the ground-state case, Eq. (2), with the static dielectric constant replaced by its high-frequency counterpart, $\bar{\epsilon} = \epsilon_\infty$, as illustrated in Fig. 3. For example, for liquid water at 298 K, $\epsilon_0 = 78.5$ and $\epsilon_\infty = 1.776$,[16,19] and the drop between ϵ_∞ and 1 is therefore much smaller than between ϵ_0 and 1.

2. Dynamic linear-response equations

In order to describe the dynamical response of a system within TDDFT[37,38] using the dielectric SCCS model, we need to linearize the latter with respect to the strength of the perturbation. Following the derivation presented in Ref. 25 in the case of a molecule in the gas phase, the Fourier transforms of the response KS orbitals, $\tilde{\varphi}'_v(\mathbf{r},\omega)$, satisfy the equations:

$$\begin{aligned}(\hat{H}^\circ_{\mathrm{KS}} - \varepsilon^\circ_v - \omega)\tilde{\varphi}'_v(\mathbf{r},\omega) + \hat{P}_c\tilde{V}'_{\mathrm{int}}(\mathbf{r},\omega)\varphi^\circ_v(\mathbf{r}) \\ = -\hat{P}_c\tilde{V}'_{\mathrm{ext}}(\mathbf{r},\omega)\varphi^\circ_v(\mathbf{r}),\end{aligned} \tag{19}$$

$$\begin{aligned}(\hat{H}^\circ_{\mathrm{KS}} - \varepsilon^\circ_v + \omega)\tilde{\varphi}'^{\,*}_v(\mathbf{r},-\omega) + \hat{P}_c\tilde{V}'_{\mathrm{int}}(\mathbf{r},\omega)\varphi^\circ_v(\mathbf{r}) \\ = -\hat{P}_c\tilde{V}'_{\mathrm{ext}}(\mathbf{r},\omega)\varphi^\circ_v(\mathbf{r}),\end{aligned} \tag{20}$$

where $\hat{P}_c = \sum_c |\varphi^\circ_c\rangle\langle\varphi^\circ_c| = 1 - \sum_v |\varphi^\circ_v\rangle\langle\varphi^\circ_v|$ is the projector over the unperturbed empty-state manifold,

$$\tilde{V}'_{\mathrm{ext}}(\mathbf{r},\omega) = -\mathbf{E}(\omega)\cdot\mathbf{r} \tag{21}$$

is the Fourier transform of the *external* perturbation induced by a homogeneous electric field and

$$\tilde{V}'_{\mathrm{int}}(\mathbf{r},\omega) = \tilde{V}'_{\mathrm{e}}(\mathbf{r},\omega) + \tilde{V}'_{\mathrm{p}}(\mathbf{r},\omega) + \tilde{V}'_{\epsilon}(\mathbf{r},\omega) + \tilde{V}'_{\mathrm{XC}}(\mathbf{r},\omega) \tag{22}$$

is the Fourier transform of the response of the *internal* contribution to the KS potential. Equations (19) and (20) describe resonant and antiresonant contributions to the charge-density response, respectively.

The response of the Hartree potential of the solute is

$$\tilde{V}'_{\mathrm{e}}(\mathbf{r},\omega) = \int \frac{\tilde{n}'_{\mathrm{e}}(\mathbf{r}',\omega)}{|\mathbf{r}-\mathbf{r}'|}\,d\mathbf{r}', \tag{23}$$

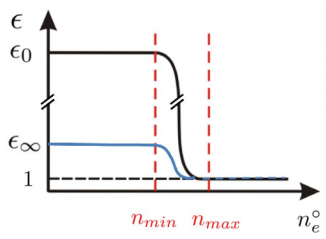

FIG. 3. Schematic illustration of the ground-state (black line) and response (blue line) dielectric functions as functions of the ground-state electronic density $n^\circ_{\mathrm{e}}(\mathbf{r})$ [see Eqs. (2) and (3)]. Here, ϵ_0 and ϵ_∞ are the static and optical dielectric constants of the solvent, respectively, and n_{min} and n_{max} are the fitting parameters of the SCCS model which control the smoothness of the interface between the solute and the solvent. The vertical scaling in the figure is not respected for a clearer visual demonstration.

where the response electronic density reads

$$\tilde{n}'_{\mathrm{e}}(\mathbf{r},\omega) = 2\sum_{v=1}^{N_v}\varphi^\circ_v(\mathbf{r})\big(\tilde{\varphi}'^{\,*}_v(\mathbf{r},-\omega) + \tilde{\varphi}'_v(\mathbf{r},\omega)\big), \tag{24}$$

and the reality of ground-state KS orbitals in time-reversal invariant systems has been used. The response XC potential reads

$$\tilde{V}'_{\mathrm{XC}}(\mathbf{r},\omega) = \int \kappa_{\mathrm{XC}}(\mathbf{r},\mathbf{r}';\omega)\,\tilde{n}'_{\mathrm{e}}(\mathbf{r}',\omega)\,d\mathbf{r}', \tag{25}$$

where the XC kernel $\kappa_{\mathrm{XC}}(\mathbf{r},\mathbf{r}';\omega)$ is the functional derivative of the ground-state XC potential, Eq. (17), with respect to its charge-density argument, which is assumed to be independent of frequency in the adiabatic DFT approximation. The response polarization potential is

$$\tilde{V}'_{\mathrm{p}}(\mathbf{r},\omega) = \int \frac{\tilde{n}'_{\mathrm{p}}(\mathbf{r}',\omega)}{|\mathbf{r}-\mathbf{r}'|}\,d\mathbf{r}', \tag{26}$$

where the response polarization density is

$$\tilde{n}'_{\mathrm{p}}(\mathbf{r},\omega) = \frac{1}{4\pi}\nabla\ln\epsilon(\mathbf{r})\cdot\nabla\tilde{V}'_{\mathrm{tot}}(\mathbf{r},\omega) - \frac{\epsilon(\mathbf{r})-1}{\epsilon(\mathbf{r})}\,\tilde{n}'_{\mathrm{e}}(\mathbf{r},\omega), \tag{27}$$

$\tilde{V}'_{\mathrm{tot}}(\mathbf{r},\omega) = \tilde{V}'_{\mathrm{e}}(\mathbf{r},\omega) + \tilde{V}'_{\mathrm{p}}(\mathbf{r},\omega)$ being the total electrostatic response potential. $\epsilon(\mathbf{r})$ is the response dielectric function, Eq. (1), which should depend on frequency through the dielectric constant of the solvent, $\bar{\epsilon}(\omega)$. Following the arguments of Sec. II B 1, we assume that it is actually frequency-independent and set it $\bar{\epsilon}(\omega) = \epsilon_\infty$. The response polarization potential, $\tilde{V}'_{\mathrm{p}}(\mathbf{r},\omega)$, is computed from Eq. (26), i.e., by solving a Poisson equation for the response polarization density, $\tilde{n}'_{\mathrm{p}}(\mathbf{r},\omega)$, which is in turn computed iteratively in the very same way as the ground-state polarization potential is obtained from the corresponding density in Sec. V of Ref. 9.

By linearizing the interface potential of the form of Eq. (16), we obtain

$$\tilde{V}'_{\epsilon}(\mathbf{r},\omega) = -\frac{1}{4\pi}\nabla V^\circ_{\mathrm{tot}}(\mathbf{r})\cdot\nabla\tilde{V}'_{\mathrm{tot}}(\mathbf{r},\omega)\frac{d\eta(n,\epsilon_\infty)}{dn}\Big|_{n=n^\circ_e(\mathbf{r})}, \tag{28}$$

where the reality of the unperturbed and response total potentials in the time domain has been used to set $\tilde{V}'^{\,*}_{\mathrm{tot}}(\mathbf{r},-\omega) = \tilde{V}'_{\mathrm{tot}}(\mathbf{r},\omega)$.

C. The Liouville approach to TDDFpT within the SCCS model

1. Linearization of the SCCS model

The Liouville approach to TDDFpT[25–27,39] is based on the linear superoperator equation for the response density matrix

$$(\omega - \mathcal{L})\cdot\tilde{\rho}'_{\mathrm{e}}(\omega) = [\tilde{V}'_{\mathrm{ext}}(\omega),\hat{\rho}^\circ_{\mathrm{e}}], \tag{29}$$

where $\hat{\rho}^\circ_{\mathrm{e}}$ is the ground-state density matrix, $\tilde{\rho}'_{\mathrm{e}}(\omega)$ is the response density matrix, and $\mathcal{L}$ is the Liouvillian superoperator, which, in the SCCS model, reads

$$\begin{aligned}\mathcal{L}\cdot\tilde{\rho}'_{\mathrm{e}}(\omega) \doteq [\hat{H}^\circ_{\mathrm{KS}},\tilde{\rho}'_{\mathrm{e}}(\omega)] + [\tilde{V}'_{\mathrm{e}}(\omega),\hat{\rho}^\circ_{\mathrm{e}}] \\ + [\tilde{V}'_{\mathrm{XC}}(\omega),\hat{\rho}^\circ_{\mathrm{e}}] + [\tilde{V}'_{\mathrm{p}}(\omega),\hat{\rho}^\circ_{\mathrm{e}}] + [\tilde{V}'_{\epsilon}(\omega),\hat{\rho}^\circ_{\mathrm{e}}].\end{aligned} \tag{30}$$

The response potentials appearing in Eq. (30) are defined in Sec. II B 2. The first three commutators in Eq. (30) are

related to the solute and appear in the Liouville equation for the molecule in the gas phase as well, while the last two are specific to the SCCS treatment of the solvent. Quantum Liouville equation (29) is equivalent to Eqs. (19) and (20). The ground-state density matrix in the coordinate representation reads

$$\rho^{\circ}_{\mathrm{e}}(\mathbf{r},\mathbf{r}') = 2\sum_{v}^{N_v}\varphi^{\circ}_{v}(\mathbf{r})\varphi^{\circ}_{v}(\mathbf{r}'), \tag{31}$$

and the corresponding expression for the linear-response density matrix is[25]

$$\tilde{\rho}'_{\mathrm{e}}(\mathbf{r},\mathbf{r}';\omega) = 2\sum_{v=1}^{N_v}\left[\varphi^{\circ}_{v}(\mathbf{r})\tilde{\varphi}'^{\,*}_{v}(\mathbf{r}',-\omega) + \tilde{\varphi}'_{v}(\mathbf{r},\omega)\varphi^{\circ}_{v}(\mathbf{r}')\right], \tag{32}$$

where the response orbitals $\tilde{\varphi}'_{v}(\mathbf{r},\omega)$ and $\tilde{\varphi}'^{\,*}_{v}(\mathbf{r},-\omega)$ satisfy Eqs. (19) and (20), respectively, and the ground-state KS orbitals $\varphi^{\circ}_{v}(\mathbf{r})$ are assumed to be real. The diagonal of the ground-state and response density matrices are the electronic ground-state and response charge-density distributions of the solute, respectively: $\rho^{\circ}_{\mathrm{e}}(\mathbf{r},\mathbf{r}) = n^{\circ}_{\mathrm{e}}(\mathbf{r})$ and $\tilde{\rho}'_{\mathrm{e}}(\mathbf{r},\mathbf{r};\omega) = \tilde{n}'_{\mathrm{e}}(\mathbf{r},\omega)$, given by Eqs. (14) and (24).

The absorption coefficient is proportional to the product of the frequency times the imaginary part of the dynamical polarizability, which according to Refs. 25 and 26 reads

$$\alpha_{ij} \equiv -\left(\hat{r}_i,(\omega-\mathcal{L})^{-1}\cdot[\hat{r}_j,\hat{\rho}^{\circ}_{\mathrm{e}}]\right), \tag{33}$$

where $\hat{r}_i$ indicates the i-th Cartesian component of the position operator, $(\cdot,\cdot)$ denotes a scalar product defined in the manifold of linear operators, $\left(\hat{A},\hat{B}\right) \doteq \mathrm{Tr}\left(\hat{A}^{\dagger}\hat{B}\right)$, and $(\omega-\mathcal{L})^{-1}$ is the resolvent of the Liouvillian superoperator, Eq. (30). The so-called *standard batch representation* (SBR)[25,26,39] allows one to represent the response density matrix, and hence to compute molecular polarizabilities, without making any reference to the empty electronic states. In the SBR, the response density matrix is defined by two *batches* of orbitals, $\hat{\rho}' \sim (q,p)$,

$$q_v(\mathbf{r}) = \frac{1}{2}\left(\tilde{\varphi}'_{v}(\mathbf{r},\omega) + \tilde{\varphi}^{*}_{v}(\mathbf{r}',-\omega)\right), \tag{34}$$

$$p_v(\mathbf{r}) = \frac{1}{2}\left(\tilde{\varphi}'_{v}(\mathbf{r},\omega) - \tilde{\varphi}^{*}_{v}(\mathbf{r}',-\omega)\right), \tag{35}$$

in terms of which the electronic response charge-density, Eq. (24), is

$$\tilde{n}'_{\mathrm{e}}(\mathbf{r},\omega) = 4\sum_{v}\varphi^{\circ}_{v}(\mathbf{r})q_v(\mathbf{r}). \tag{36}$$

By analogy, all single-particle quantum mechanical operators can be represented in the SBR, and the Liouvillian takes the form

$$\mathcal{L} = \begin{pmatrix} 0 & \mathcal{D} \\ \mathcal{D}+\mathcal{K}_{\mathrm{m}}+\mathcal{K}_{\mathrm{s}} & 0 \end{pmatrix}, \tag{37}$$

where the superoperators $\mathcal{D}$, $\mathcal{K}_{\mathrm{m}}$, and $\mathcal{K}_{\mathrm{s}}$ are defined by their action on batches of orbitals. For example, the representation of the non-interacting component of the Liouvillian is

$$\mathcal{D}\{q_v(\mathbf{r})\} = \left\{(\hat{H}^{\circ}_{\mathrm{KS}} - \varepsilon^{\circ}_{v})q_v(\mathbf{r})\right\}. \tag{38}$$

The expressions for $\mathcal{K}_{\mathrm{m}}\{q_v(\mathbf{r})\}$ and $\mathcal{K}_{\mathrm{s}}\{q_v(\mathbf{r})\}$, which are the *molecular* (solute) and *solvent* contributions to the interaction component of the Liouvillian, in terms of $q_v(\mathbf{r})$, are rather cumbersome, and, anyway, of little practical use. In practice, the action of the superoperators $\mathcal{K}_{\mathrm{m}}$ and $\mathcal{K}_{\mathrm{s}}$ on batches of response orbitals is treated by first calculating the response electronic and polarization densities, $\tilde{n}'_{\mathrm{e}}(\mathbf{r},\omega)$ and $\tilde{n}'_{\mathrm{p}}(\mathbf{r},\omega)$, then by computing the corresponding response potentials, and finally by letting them act onto ground-state orbitals according to the expressions

$$\mathcal{K}_{\mathrm{m}}\{q_v(\mathbf{r})\} = \left\{\hat{P}_c\left[\tilde{V}'_{\mathrm{e}}(\mathbf{r},\omega) + \tilde{V}'_{\mathrm{XC}}(\mathbf{r},\omega)\right]\varphi^{\circ}_{v}(\mathbf{r})\right\}, \tag{39}$$

$$\mathcal{K}_{\mathrm{s}}\{q_v(\mathbf{r})\} = \left\{\hat{P}_c\left[\tilde{V}'_{\mathrm{p}}(\mathbf{r},\omega) + \tilde{V}'_{\epsilon}(\mathbf{r},\omega)\right]\varphi^{\circ}_{v}(\mathbf{r})\right\}. \tag{40}$$

Once the Liouvillian is represented in the SBR, Eq. (37), a Lanczos recursive algorithm can be conveniently applied to obtain dynamical polarizability (33) over a wide energy range, as explained in Refs. 25–27. Alternatively, if only a few discrete excited states are required, it may be convenient to obtain them from the solution of the Casida eigenvalue equation[40] that results from Eq. (29) when the perturbation acting on the solvated molecule vanishes, thus describing free oscillations of the system. Using the SBR representation of the Liouvillian, the Casida equation can be conveniently solved without having ever to compute any virtual orbitals using powerful iterative eigenvalue techniques, such as, e.g., the Davidson-like solver proposed in Ref. 27.

2. Hybrid XC functionals

The methodology presented so far is appropriate to local (such as LDA[35]) or semilocal (such as GGA[41]) XC functionals, which are known to underestimate systematically quasi-particle gaps and fail to properly predict Rydberg states in molecules, excitons in insulators, as well as charge-transfer excitations in general.[42,43] These failures can be addressed to a large extent by hybrid functionals,[44] such as B3LYP,[45,46] or PBE0,[47] which open the gap and generally result in a better agreement of the computed optical properties with experiments.

In hybrid functionals, a fraction of the local exchange potential is replaced by a same fraction of the non-local Fock potential. In PBE0, for instance, the action of the ground-state XC potential onto a generic wavefunction $\psi(\mathbf{r})$ is defined as

$$\hat{V}^{\circ}_{\mathrm{XC}}\psi(\mathbf{r}) = \int v^{\circ}_{\mathrm{XC}}(\mathbf{r},\mathbf{r}')\psi(\mathbf{r}')d\mathbf{r}', \tag{41}$$

where the integral kernel v°_{XC} reads

$$v^{\circ}_{\mathrm{XC}}(\mathbf{r},\mathbf{r}') = V^{\circ\alpha}_{\mathrm{XC}}(\mathbf{r})\delta(\mathbf{r}-\mathbf{r}') - \alpha\,\frac{\rho^{\circ}_{\mathrm{e}}(\mathbf{r},\mathbf{r}')}{|\mathbf{r}-\mathbf{r}'|}, \tag{42}$$

$$V^{\circ\alpha}_{\mathrm{XC}}(\mathbf{r}) = (1-\alpha)V^{\circ\mathrm{PBE}}_{\mathrm{X}}(\mathbf{r}) + V^{\circ\mathrm{PBE}}_{\mathrm{C}}(\mathbf{r}), \tag{43}$$

$\alpha = 1/4$, $V^{\circ\mathrm{PBE}}_{\mathrm{C}}(\mathbf{r})$ and $V^{\circ\mathrm{PBE}}_{\mathrm{X}}(\mathbf{r})$ are the PBE correlation and exchange potentials, respectively,[47] and $\rho^{\circ}_{\mathrm{e}}(\mathbf{r},\mathbf{r}')$ is the ground-state density matrix of Eq. (31).

In linear-response theory, the response XC potential must be modified in a way similar to the ground-state case, Eqs. (41) and (42). Namely,

$$\hat{V}'_{\mathrm{XC}}(\omega)\psi(\mathbf{r}) = \int \tilde{v}'_{\mathrm{XC}}(\mathbf{r},\mathbf{r}';\omega)\psi(\mathbf{r}')d\mathbf{r}', \tag{44}$$

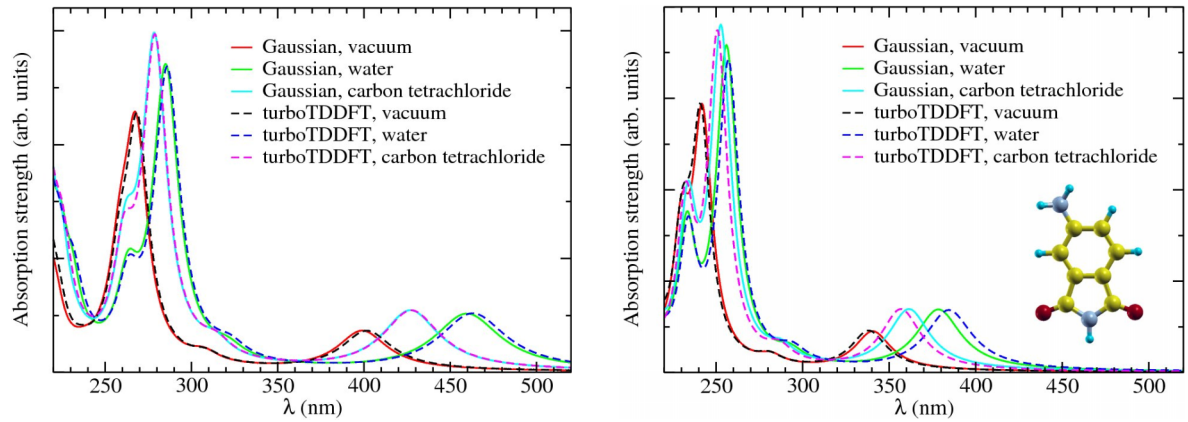

FIG. 4. Comparison of the absorption spectra of the 4-AP molecule in vacuum, water, and carbon tetrachloride, using the GAUSSIAN code and the PCM model on one hand and the `turboTDDFT` code and the SCCS model on the other hand. Panel (a): GGA-PBE XC functional. Panel (b): B3LYP XC functional.

where the integral kernel $\tilde{v}'_{\rm XC}$ reads

$$\tilde{v}'_{\rm XC}(\mathbf{r},\mathbf{r}';\omega) = \tilde{V}'^{\,\alpha}_{\rm XC}(\mathbf{r},\omega)\delta(\mathbf{r}-\mathbf{r}') - \alpha\,\frac{\tilde{\rho}'_{\rm e}(\mathbf{r},\mathbf{r}';\omega)}{|\mathbf{r}-\mathbf{r}'|}, \quad (45)$$

where the local response potential $\tilde{V}'^{\,\alpha}_{\rm XC}(\mathbf{r},\omega)$ is similar to Eq. (43) and $\tilde{\rho}'_{\rm e}(\mathbf{r},\mathbf{r}';\omega)$ is the response density matrix of Eq. (32).

Similarly to Ref. 27, Liouvillian (37) in the SBR reads

$$\mathcal{L} = \begin{pmatrix} 0 & \mathcal{D} - \alpha(\mathcal{K}^{\rm 1d} - \mathcal{K}^{\rm 2d}) \\ \mathcal{D} + \mathcal{K}^{\alpha}_{\rm m} + \mathcal{K}_{\rm s} - \alpha(\mathcal{K}^{\rm 1d} + \mathcal{K}^{\rm 2d}) & 0 \end{pmatrix}, \quad (46)$$

where

$$\mathcal{K}^{\alpha}_{\rm m}\{q_v(\mathbf{r})\} = \{\hat{P}_c[\tilde{V}'_{\rm e}(\mathbf{r},\omega) + \tilde{V}'^{\,\alpha}_{\rm XC}(\mathbf{r},\omega)]\varphi^{\circ}_v(\mathbf{r})\}, \quad (47)$$

$$\mathcal{K}^{\rm 1d}\{q_v(\mathbf{r})\} = \Big\{2\hat{P}_c \sum_{v'} \int \frac{\varphi^{\circ}_v(\mathbf{r}')\varphi^{\circ}_{v'}(\mathbf{r}')}{|\mathbf{r}-\mathbf{r}'|} d\mathbf{r}' q_{v'}(\mathbf{r})\Big\}, \quad (48)$$

$$\mathcal{K}^{\rm 2d}\{q_v(\mathbf{r})\} = \Big\{2\hat{P}_c \sum_{v'} \int \frac{\varphi^{\circ}_v(\mathbf{r}')q_{v'}(\mathbf{r}')}{|\mathbf{r}-\mathbf{r}'|} d\mathbf{r}' \varphi^{\circ}_{v'}(\mathbf{r})\Big\}, \quad (49)$$

the factor of 2 is due to spin degeneracy and $\mathcal{K}_{\rm s}$ is given by Eq. (40). Note that the solvent contribution to the response potential, whose nature is essentially electrostatic, is unaffected by the use of hybrid, rather than (semi-) local, XC functionals, and the implementation of the dielectric SCCS model is largely independent on the XC functional of choice.

The calculation of molecular polarizabilities through Eq. (33) requires the evaluation of the action of the dipole operator onto the unperturbed KS molecular orbitals. The usual way of performing this task in periodic-boundary conditions is via the velocity operator, which is in turn evaluated through the commutator between the Hamiltonian and dipole operators.[48] When hybrid functionals are used, this commutator has also contributions from the Fock component of the XC potential. Although these contributions can be computed in principle, the dielectric SCCS model effectively maps the solvent-solute system onto a finite system, and the dipole operator can be treated more simply in real space as explained in Ref. 27, which we do in the present work.

III. IMPLEMENTATION AND BENCHMARK

The methodology described above has been implemented in the `turboTDDFT`[27,39] component of the QUANTUM ESPRESSO suite of computer codes[31] and is scheduled to be distributed in one of its forthcoming releases.

In order to validate our approach, we consider 3 neutral molecules: 4-AP, $C_8H_6N_2O_2$, consisting of 18 atoms; alizarin, $C_{14}H_8O_4$, consisting of 26 atoms; and cyanin, $C_{21}H_{20}O_{11}$, consisting of 52 atoms (see the insets of Figs. 4(b), 5(b), and 6(b)). For these molecules, the new methodology is benchmarked against PCM calculations performed with the GAUSSIAN code,[32,49,50] and resulting in a remarkable agreement between the two sets of calculations. Our purpose here is not to analyze the optical properties of these molecules or to make any comparison with experiments, but to demonstrate the correctness of our implementation and the consistency of the methodology on which it is based with the by now well established PCM.

A. Technical details

Exchange-correlation effects have been approximated using both GGA (PBE[41]) and hybrid (B3LYP[45,46]) energy functionals. The implicit solvent was simulated using the static and optical dielectric constants of liquid water at 298 K, $\epsilon_0 = 78.5$ and $\epsilon_\infty = 1.776$,[16,19] and of carbon tetrachloride, $\epsilon_0 = 2.2$ and $\epsilon_\infty = 2.129$.[49] For the sake of validation of our approach for various solvents, we present the spectra of all three molecules in water and only of the simplest of them, 4-AP, in carbon tetrachloride.[51] Various other solvents can be used with the corresponding values of the static and optical dielectric constants. All spectra were convoluted with a Lorentzian function with a broadening parameter of 0.01 Ry.

Calculations with the `turboTDDFT` code have been performed using PBE ultrasoft[52] and BLYP norm-conserving[53] pseudopotentials from the QUANTUM ESPRESSO pseudopotential library,[54] in the GGA-PBE and B3LYP cases, respectively. Periodic boundary conditions were imposed on the molecular orbitals by using $18.5 \times 20.0 \times 16.0$ Å^3, $18.5 \times 24.0 \times 16.0$ Å^3,

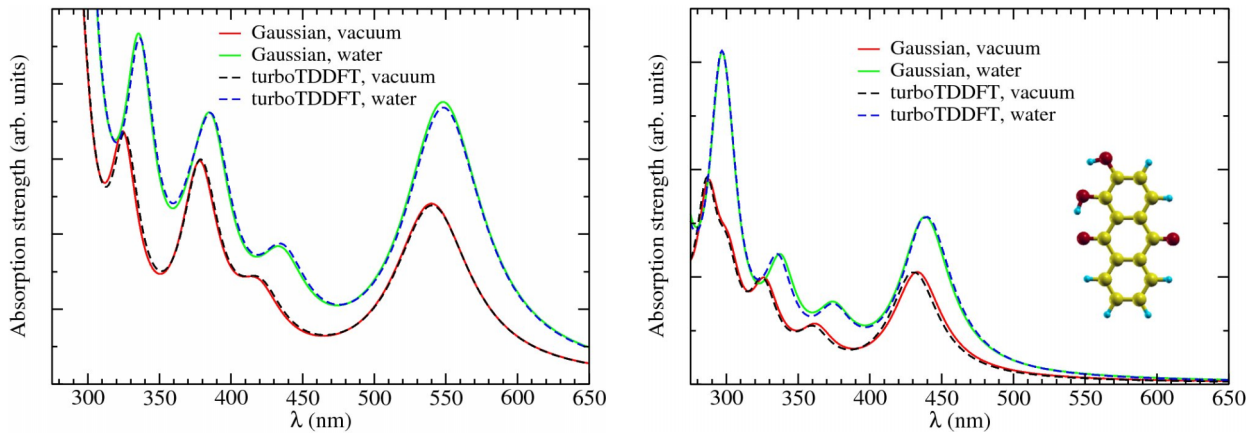

FIG. 5. Comparison of the optical absorption spectra of the alizarin molecule in vacuum and in water, using the GAUSSIAN code and the PCM model on one hand and the `turboTDDFT` code and the SCCS model on the other hand. Panel (a): GGA-PBE XC functional. Panel (b): B3LYP XC functional.

and 20.0 × 20.0 × 20.0 Å^3 supercells for 4-AP, alizarin, and cyanin, respectively. KS orbitals have been expanded in PWs up to a kinetic energy cutoff of 25 and 50 Ry when using ultrasoft and norm-conserving pseudopotentials, respectively, and in both cases, PWs up to 200 Ry have been retained to expand the electronic charge-density distribution and potentials. We have used a reduced cutoff of 50 Ry for the exact exchange potentials of Sec. II C 2 in calculations with hybrid functionals, as explained in Ref. 27. The geometries of all three molecules were optimized in vacuum and in the implicit solvent using the dielectric SCCS model, both with GGA-PBE and B3LYP functionals. In all cases, the convergence of both the geometrical and spectral properties of the molecule with respect to the relevant numerical details (size and shape of the supercell, size of the PW basis set, number of Lanczos/Davidson iterations, etc.) was carefully checked.

The inclusion of polarization and diffuse functions in the Gaussian basis set was necessary to obtain fully converged GAUSSIAN calculations. The triple-zeta `aug-cc-pVTZ` basis set was used for 4-AP and the double-zeta `aug-cc-pVDZ` basis set was used for alizarin and cyanin. GAUSSIAN calculations have been performed at the geometries optimized with the QUANTUM ESPRESSO package, as described above.

B. Validation

In Figs. 4-6, we compare the TDDFT absorption spectra of 4-AP, alizarin, and cyanin, as computed in vacuum and in implicit solvents with the `turboTDDFT` (SCCS) and GAUSSIAN (PCM) codes. As expected, adoption of a hybrid functional results in the opening (blue shift) of the optical gap with respect to GGA. The agreement between SCCS and PCM results is excellent in all cases, witnessing to a correct implementation of our newly proposed SCCS methodology, as well as to its consistency with the popular PCM technique. In particular, spectra of the 4-AP molecule in water and in carbon tetrachloride solvents agree remarkably with the corresponding reference PCM spectra (see Fig. 4), which confirms the validity of our approach for various solvents. The minor differences between `turboTDDFT` and GAUSSIAN

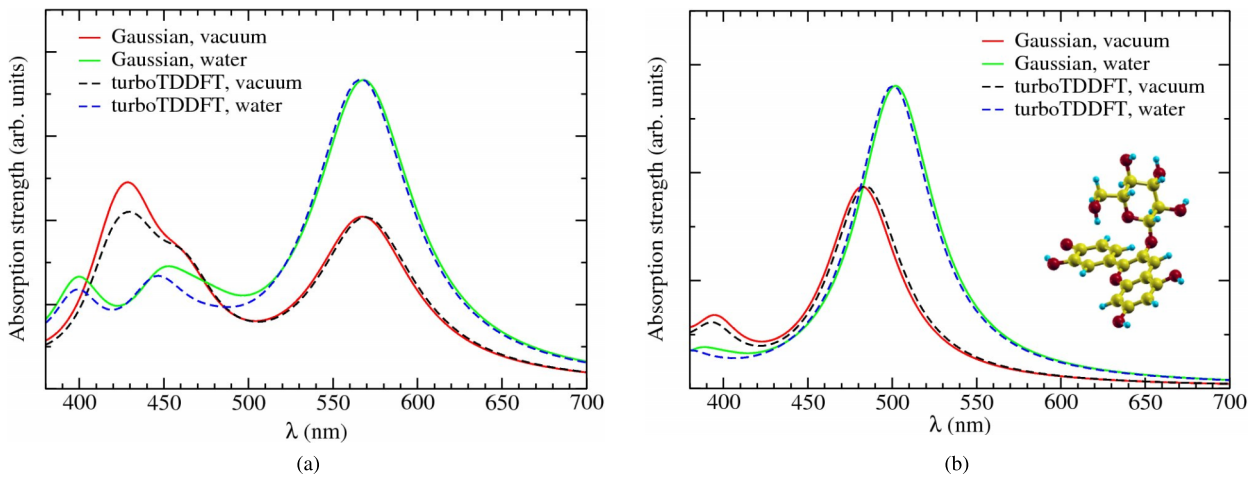

FIG. 6. Comparison of the optical absorption spectra of the cyanin molecule in vacuum and in water, using the GAUSSIAN code and the PCM model on one hand and the `turboTDDFT` code and the SCCS model on the other hand. Panel (a): GGA-PBE XC functional. Panel (b): B3LYP XC functional.

results (particularly, in the short-wavelength portion of the spectrum in cyanin) likely depend on the pseudopotential approximation adopted in the first case, as well as on some residual deficiencies in the basis set in the latter. *Solvatochromic* effects[55] (i.e., the dependence of the optical spectra on the solvent) result in a red shift of the relevant spectra features. The magnitude of the solvatochromic shifts in cyanin (which is a more complex and flexible molecule than 4-AP and alizarin) results from a combination of static and dynamical effects, the first being due to the different equilibrium geometries that the molecule has in vacuum and in solution, whereas the latter specifically depends on the screening of electronic transitions that is the main focus of the present work. Disentangling these two effects is out of the scope of the present paper and will be the subject of further research.

IV. CONCLUSIONS

The optical properties of complex molecular systems in solution differ from those in the gas phase in two distinct ways. On the one hand, the solvent acts as a thermal bath, allowing thermal fluctuations to indirectly affect the absorption of light from the molecule, via the geometrical distortions induced by them. Explicit solvent simulations have shown that a proper account of these thermal effects is crucial to understand the optical and chromatic properties of some natural dyes and can effectively be modeled by *ab initio* molecular dynamics.[1] The residual dielectric effects on the excitation process, though not as important, are not negligible, but they are very expensive to simulate through explicit solvent models. We think that the methodology presented in this paper will constitute a key ingredient of a multi-scale simulation strategy combining an explicit account of thermal effects on the molecular geometry with an implicit account of dielectric effects on the excitation process. In this paper, we have provided a detailed technical validation of the newly proposed methodology. A validation of the physical approximations on which it is based will call for a thorough comparison of explicit- and implicit-solvent TDDFT calculations with each other, on one hand and with experiment, on the other.

ACKNOWLEDGMENTS

This work was partially supported by *Mars Chocolate North America LLC* (I.T., A.B., and S.B.) and *PASC ENVIRON* (O.A. and N.M.). Computer resources were provided by the CINECA supercomputing center (Italy) at their Fermi BG/Q machine through *PRACE* Grant No. 2013081532, *Chromatology*. Technical support from Carlo Cavazzoni and Fabio Affinito at CINECA is gratefully acknowledged.

[1]O. B. Malcioglu, A. Calzolari, R. Gebauer, D. Varsano, and S. Baroni, J. Am. Chem. Soc. **133**, 15425 (2011).
[2]J. Tomasi, B. Mennucci, and R. Cammi, Chem. Rev. **105**, 2999 (2005).
[3]S. Miertus, E. Scrocco, and J. Tomasi, Chem. Phys. **55**, 117 (1981).
[4]A. Fortunelli and J. Tomasi, Chem. Phys. Lett. **231**, 34 (1994).
[5]B. Mennucci and J. Tomasi, J. Chem. Phys. **106**, 5151 (1997).
[6]V. Barone, M. Cossi, and J. Tomasi, J. Chem. Phys. **107**, 3210 (1997).
[7]B. Mennucci, J. Phys. Chem. Lett. **1**, 1666 (2010).
[8]A. Klamt and G. Schüürmann, J. Chem. Soc., Perkin Trans. 2 **1993**, 799.
[9]O. Andreussi, I. Dabo, and N. Marzari, J. Chem. Phys. **136**, 064102 (2012).
[10]C. Dupont, O. Andreussi, and N. Marzari, J. Chem. Phys. **139**, 214110 (2013).
[11]O. Andreussi and N. Marzari, Phys. Rev. B **90**, 245101 (2014).
[12]J.-L. Fattebert and F. Gygi, J. Comput. Chem. **23**, 662 (2002).
[13]J.-L. Fattebert and F. Gygi, Int. J. Quantum Chem. **93**, 139 (2003).
[14]D. A. Scherlis, J.-L. Fattebert, F. Gygi, M. Cococcioni, and N. Marzari, J. Chem. Phys. **124**, 074103 (2006).
[15]J. Dziedzic, H. Helal, C.-K. Skylaris, A. Mostofi, and M. Payne, Europhys. Lett. **95**, 43001 (2011).
[16]B. Mennucci, A. Toniolo, and C. Cappelli, J. Chem. Phys. **111**, 7197 (1999).
[17]M. Cossi and V. Barone, J. Chem. Phys. **112**, 2427 (2000).
[18]R. Cammi, S. Corni, B. Mennucci, and J. Tomasi, J. Chem. Phys. **122**, 104513 (2005).
[19]R. Cammi and B. Mennucci, J. Chem. Phys. **110**, 9877 (1999).
[20]M. Cossi and V. Barone, J. Chem. Phys. **115**, 4708 (2001).
[21]*Fundamentals of Time-Dependent Density Functional Theory*, Lecture Notes in Physics, edited by M. A. L. Marques, N. T. Maitra, F. M. S. Nogueira, E. K. U. Gross, and A. Rubio (Springer-Verlag, Berlin, Heidelberg, 2012), Vol. 837.
[22]R. Cammi, J. Chem. Phys. **131**, 164104 (2009).
[23]R. Cammi, R. Fukuda, M. Ehara, and H. Nakatsuji, J. Chem. Phys. **133**, 024104 (2010).
[24]B. Walker, A. M. Saitta, R. Gebauer, and S. Baroni, Phys. Rev. Lett. **96**, 113001 (2006).
[25]D. Rocca, R. Gebauer, Y. Saas, and S. Baroni, J. Chem. Phys. **128**, 154105 (2008).
[26]S. Baroni and R. Gebauer, "The Liouville-Lanczos approach to time-dependent density-functional (perturbation) theory," in *Fundamentals of Time-Dependent Density Functional Theory*, edited by M. A. L. Marques, N. T. Maitra, F. M. S. Nogueira, E. K. U. Gross, and A. Rubio (Springer-Verlag, Berlin, Heidelberg, 2012), Vol. 837, Chap. 19, pp. 375–390.
[27]X. Ge, S. J. Binnie, D. Rocca, R. Gebauer, and S. Baroni, Comput. Phys. Commun. **185**, 2080 (2014).
[28]D. H. Douma, B. M'Passi-Mabiala, and R. Gebauer, J. Chem. Phys. **137**, 154314 (2012).
[29]B. Mennucci, J. Am. Chem. Soc. **124**, 1506 (2002).
[30]J. Kongsted and B. Mennucci, J. Phys. Chem. A **111**, 9890 (2007).
[31]P. Giannozzi, S. Baroni, N. Bonini, M. Calandra, R. Car, C. Cavazzoni, D. Ceresoli, G. Chiarotti, M. Cococcioni, I. Dabo *et al.*, J. Phys.: Condens. Matter **21**, 395502 (2009); see also http://www.quantum-espresso.org.
[32]The calculations were done with GAUSSIAN 09 (Ref. 49), but using the version of PCM which was the default in GAUSSIAN 03 (Ref. 50), as specified by the keyword `g03defaults`. Note, only the electrostatic effects were included in the PCM calculation.
[33]M. Cococcioni, F. Mauri, G. Ceder, and N. Marzari, Phys. Rev. Lett. **94**, 145501 (2005).
[34]P. Hohenberg and W. Kohn, Phys. Rev. **136**, B864 (1964).
[35]W. Kohn and L. Sham, Phys. Rev. **140**, A1133 (1965).
[36]V. M. Sanchez, M. Sued, and D. A. Scherlis, J. Chem. Phys. **131**, 174108 (2009).
[37]E. Runge and E. Gross, Phys. Rev. Lett. **52**, 997 (1984).
[38]E. K. U. Gross, J. F. Dobson, and M. Petersilka, *Density Functional Theory of Time-Dependent Phenomena*, Topics in Current Chemistry (Springer-Verlag, Berlin, 1996).
[39]O. B. Malcioglu, R. Gebauer, D. Rocca, and S. Baroni, Comput. Phys. Commun. **182**, 1744 (2011).
[40]M. E. Casida, *Recent Developments and Applications of Modern Density Functional Theory* (Elsevier, Amsterdam, 1996).
[41]J. P. Perdew, K. Burke, and M. Ernzerhof, Phys. Rev. Lett. **77**, 3865 (1996).
[42]A. Dreuw, J. L. Weisman, and M. Head-Gordon, J. Chem. Phys. **119**, 2943 (2003).
[43]A. Dreuw and M. Head-Gordon, Chem. Phys. Lett. **426**, 231 (2006).
[44]A. D. Becke, J. Chem. Phys. **98**, 1372 (1993).
[45]K. Kim and K. D. Jordan, J. Phys. Chem. **98**, 10089 (1994).
[46]P. J. Stephens, F. J. Devlin, C. F. Chabalowski, and M. J. Frisch, J. Phys. Chem. **98**, 11623 (1994).

[47]C. Adamo and V. Barone, J. Chem. Phys. **110**, 6158 (1999).
[48]S. Baroni, S. de Gironcoli, A. D. Corso, and P. Giannozzi, Rev. Mod. Phys. **73**, 515 (2001).
[49]M. J. Frisch, G. W. Trucks, H. B. Schlegel, G. E. Scuseria, M. A. Robb, J. R. Cheeseman, G. Scalmani, V. Barone, B. Mennucci, G. A. Petersson *et al.*, GAUSSIAN 09, Revision C.01, Gaussian, Inc., Wallingford, CT, 2009; http://www.gaussian.com.
[50]M. J. Frisch, G. W. Trucks, H. B. Schlegel, G. E. Scuseria, M. A. Robb, J. R. Cheeseman, J. A. Montgomery, Jr., T. Vreven, K. N. Kudin, J. C. Burant *et al.*, GAUSSIAN 03, *Revision C.02*, Gaussian, Inc., Wallingford, CT, 2004; http://www.gaussian.com.
[51]For the carbon tetrachloride solvent we have used the same fitting parameters n_{min} and n_{max} (which define the cavity) as were optimized in water for 240 neutral molecules in Ref. 9.
[52]`H.pbe-rrkjus.UPF`, `O.pbe-rrkjus.UPF`, `C.pbe-rrkjus.UPF`, and `N.pbe-rrkjus.UPF`.
[53]`H.blyp-vbc.UPF`, `O.blyp-mt.UPF`, `C.blyp-mt.UPF`, and `N.blyp-mt.UPF`.
[54]See http://www.quantum-espresso.org/pseudopotentials for a pseudopotential library.
[55]A. Marini, A. Munoz-Losa, A. Biancardi, and B. Mennucci, J. Phys. Chem. B **114**, 17128 (2010).